Paleobiology, 41(2), 2015, pp. 205–225
DOI: 10.1017/pab.2014.18

When conifers took flight: a biomechanical evaluation of an imperfect evolutionary takeoff

Robert A. Stevenson, Dennis Evangelista, and Cindy V. Looy

Abstract.—*Manifera talaris*, a voltzian conifer from the late early to middle Permian (ca. 270 Ma) of Texas, is the earliest known conifer to produce winged seeds indicative of autorotating flight. In contrast to autorotating seeds and fruits of extant plants, the ones of *M. talaris* are exceptional in that they have variable morphology. They bore two wings that produced a range of wing configurations, from seeds with two equal-sized wings to single-winged specimens, via various stages of underdevelopment of one of the wings. To examine the effects of various seed morphologies on aerodynamics and dispersal potential, we studied the flight performance of paper models of three morphotypes: symmetric double-winged, asymmetric double-winged, and single-winged. Using a high-speed camera we identified the mode of descent (plummeting, gliding, autorotation) and quantified descent speed, autorotation frequency, and other flight characteristics. To validate such modeling as an inferential tool, we compared descent of extant analogues (kauri; *Agathis australis*) with descent of similarly constructed seed models. All three seed morphotypes exhibited autorotating flight behavior. However, double-winged seeds, especially symmetric ones, failed to initiate slow autorotative descent more frequently than single-winged seeds. Even when autorotating, symmetric double-winged seeds descend faster than asymmetric double-winged ones, and descent is roughly twice as fast compared to single-winged seeds. Moreover, the relative advantage that (effectively) single-winged seeds have in slowing descent during autorotation becomes larger as seed weight increases. Hence, the range in seed wing configurations in *M. talaris* produced a wide variation in potential dispersal capacity. Overall, our results indicate that the evolutionarily novel autorotating winged seeds must have improved conifer seed dispersal, in a time when animal vectors for dispersion were virtually absent. Because of the range in wing configuration, the early evolution of autorotative flight in conifers was a functionally imperfect one, which provides us insight into the evolutionary developmental biology of autorotative seeds in conifers.

Robert A. Stevenson and Dennis Evangelista. Department of Integrative Biology, University of California, Berkeley, 3060 Valley Life Sciences Building #3140, Berkeley, California 94720, U.S.A.* *Present address: *Department of Biology, CB# 3280 Coker Hall, University of North Carolina, Chapel Hill, North Carolina 27599-3280, U.S.A.*

Cindy V. Looy. Department of Integrative Biology and Museum of Paleontology, University of California, Berkeley, 3060 Valley Life Sciences Building #3140, Berkeley, California 94720, U.S.A. E-mail: looy@berkeley.edu.

Accepted: 22 September 2014
Published online: 12 March 2015
Supplemental materials deposited at Dryad: doi:10.5061/dryad.h6289

Introduction

Background.—Plants have evolved a variety of ways to disperse their diaspores (Tiffney 1986). Each dispersal mode uses biotic and/or abiotic vectors, and often comes with a suite of associated morphological characters to promote dispersal via specific pathways (Howe and Smallwood 1982; Van der Pijl 1982). Such seed dispersal syndromes are commonly still visible in fossil remains and can thus be used to infer the dominant dispersal mode in extinct plant groups (Tiffney 1986, 2004; Eriksson et al. 2000). During the Pennsylvanian and early Permian seeds with adaptations for wind and water dispersal (anemochory and hydrochory) appeared in several lineages (Tiffney 1986, 2004). For instance, in early conifers (Voltziales) a variety of seed morphologies existed characteristic of wind dispersal (Rothwell et al. 2005). Some members of the walchian Voltziales produced seeds with integumentary-derived lateral or encircling wings (e.g., *Otovicia hypnoides*; Kerp et al. 1990; Rothwell et al. 2005). Two taxa within their sister group, the voltzian Voltziales, developed larger integumentary wings positioned toward the chalazal end of the seed (Clement-Westerhof 1984, 1987, 1988; Looy and Stevenson 2014).

The earliest conifer known to produce seeds with large wings indicative of autorotative flight, is an early/middle Permian voltzian

 0094-8373/15

conifer (Kungurian–Roadian, ca. 270 Ma) from north-central Texas (DiMichele et al. 2001; Looy and Stevenson 2014). These seeds, belonging to *Manifera talaris*, are exceptional in that they have a variable wing morphology (Fig. 1A–I). Their wing configuration ranges from two equal-sized

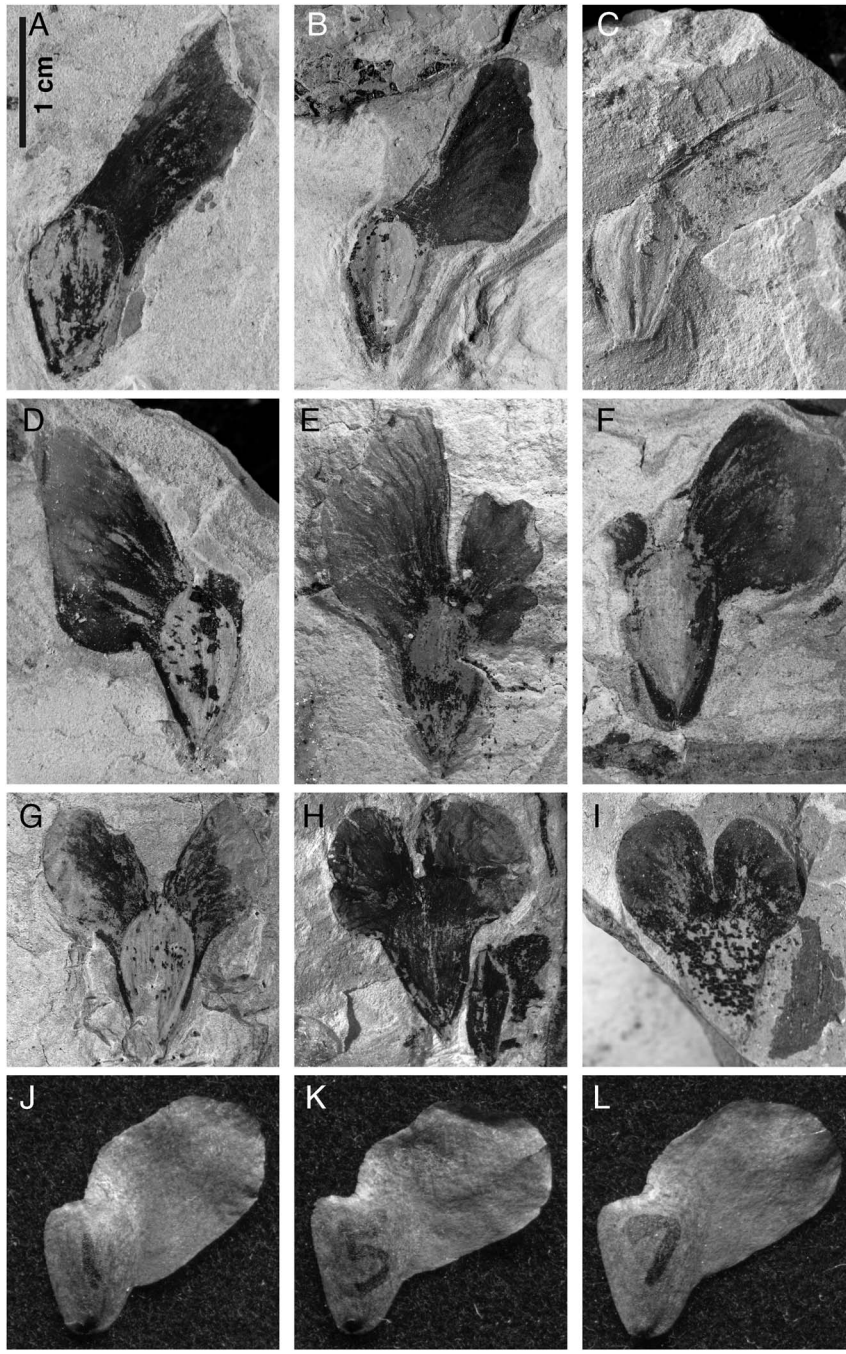

FIGURE 1. Seeds of *Manifera talaris* Looy and Stevenson (2014). All images are at the same scale. A–C, Single-winged seeds. D–F, Asymmetrical double-winged seeds. G–I, Symmetrical double-winged seeds. J–L, Functionally single-winged seeds of *Agathis australis*. USNM numbers: A, 544043; B, 544018; C, 544015; D, 544038; E, 544008; F, 543999; G, 544624; H, 544020; I, 544035. UCMP numbers: J, 254910; K, 254911; L, 254912.

wings, to (functionally) single-winged specimens via intermediate morphologies with various levels of underdevelopment of one of the wings (Looy and Stevenson 2014). The variety of seed morphotypes produced by *M. talaris* raises the question: what is the effect of wing configuration on aerodynamics and, ultimately, dispersal potential?

Studies of the aerodynamics of extant plants often use the actual seeds or fruits (Norberg 1973; Burrows 1975; Sipe and Linnerooth 1985; Azuma and Okuno 1987; Azuma and Yasuda 1989; Greene and Johnson 1990; Greene and Quesada 1992; Lentink et al. 2009; Evangelista et al. 2011; Varshney et al. 2012), but reconstructed diaspore models also are known to provide close approximations. For example, paper models have been used in studies of the limits of stability in autorotation (Yasuda and Azuma 1997) or in analogues of turbulence (Childress et al. 2006). In paleobotanical studies of seed flight, Call and Dilcher (1997) also used paper models to observe occurrence of rolling autorotation in Eocene members of the genus *Eucommia.* So far, however, no performance studies have been done on seeds with two functional wings positioned toward the chalazal end of the seed; therefore, we could only surmise their mode of descent thus far. On the basis of these previous studies, we designed a series of model tests to (1) examine the role of wing morphotype in determining flight behavior (to address the consequences of the polymorphism seen in *M. talaris*), (2) examine the interplay between wing morphotype and seed weight (which reflects the trade-offs between parental investment, dispersal range, and seedling establishment success), and (3) validate paper models by comparison with autorotating seeds of an extant conifer. We experimentally tested physical models to observe the mode of descent (common modes include plummeting, parachuting stable drag descents, straight-line stable gliding, stable helical gliding, long-axis rotation/rolling, autorotation, autorotation with sideslip; see four examples in Fig. 2), the frequencies of each mode, and other measures of autorotative flight performance (e.g., speed and descent time). We used models of *Manifera talaris* morphotypes as well as similarly shaped and sized functionally single-winged seeds of the extant kauri (*Agathis australis*; Fig 1K-L) and their models. The results of these paleobiomechanical simulations are used to explore the evolution and ecological implications of autorotating winged seeds.

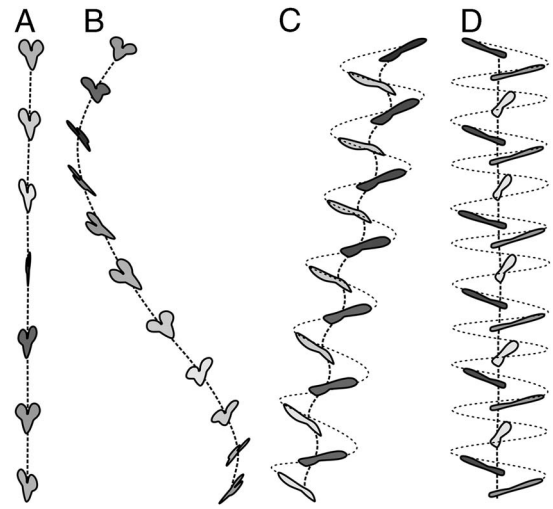

FIGURE 2. Descent modes. A, Plummeting. B, Gliding with a constant yaw turn. C, Autorotation with sideslip. D, Autorotation.

Material and Methods

Geological Setting and Localities.—The fossils studied here are from the lower part of the Pease River Group, which is latest Leonardian (Kungurian) to Wordian in age (Wardlaw 2005). Plant fossils representing the Lower Pease River Flora are preserved in mudstones of the Flowerpot Shale Member of the San Angelo Formation, at or near the contact with the overlying Blaine Formation (DiMichele et al. 2001). The assemblages are paraautochthonous and occur in channel facies within a coastal plain setting in the Midland Basin. The Lower Pease River Flora is known from seven localities in King, Knox, and Stonewall Counties, in north central Texas. The winged seed specimens for this paper are from the Buzzard Peak locality collections, and are listed under USNM collecting locality numbers 41391, 41395–41398 and 42103. Information on the exact locality is not recorded in this report, but is on file at the

U.S. National Museum of Natural History (NMNH). More information on the Lower Pease River Flora, biostratigraphy and geological setting is provided by DiMichele et al. (2001) and Looy (2007).

Fossil Plant Material.—The Lower Pease River Flora is dominated by gymnosperms and includes cordaites, ginkgophytes, cycadophytes, calamites, and walchian and voltzian conifers (DiMichele et al. 2001). The voltzian conifer that produced the winged seeds, *Manifera talaris*, belongs to the Majonicaceae (Looy and Stevenson 2014), an extinct monophyletic group of tree taxa with an orthotropic branching pattern (Rothwell et al. 2005). In this study we examined 23 dispersed *Manifera talaris* seeds in a morphometric analysis. These specimens are housed in the Paleobotanical Collections of the U.S. National Museum of Natural History, Smithsonian Institution, Washington, D.C. Illustrated or traced specimens are stored in the Paleobotanical Type and Illustrated Collections under the following USNM catalog numbers: 543998, 543999, 544000, 544003, 544004, 544008, 544009, 544015, 544018, 544020, 544021, 544024, 544029, 544030, 544033, 544035, 544038, 544040, 544043, 544622, 544623, 544624, 544625 (also see figure captions).

The seed body of the *Manifera talaris* seeds is bilaterally symmetrical, rhomboid to obovate in outline. The micropylar end varies between acute and obtuse at its apex. Extensions of the integument form two wings of variable size (Fig. 1A–I) near the chalazal end of the seeds. The wings are thicker at their base, but thin distally along the wingspan. They are oriented at approximately 35–60° relative to the seed's mediolateral axis. Wing geometries vary from irregularly oval to trapezoidal. For a more detailed description of the seeds and their ovuliferous dwarf shoots, see Looy and Stevenson (2014).

Seed Morphotypes.—We photographed the fossil seeds using a Zeiss Stemi SV 11 with a Nikon DXM1200F digital camera or a Canon EOS 5D Mark II camera with a Canon EF 100 mm Macro lens. We screened the images for completeness of the seed outline and ability to clearly differentiate the fossils from the matrix. We used ImageJ (NIH, Bethesda, MD) to determine the morphometrics of the most intact seeds. Seed body (without wings) lengths were taken along the central axis. Seed widths were measured perpendicular to the seed axis at the junction of the integument, between the lower side of wing(s) and the seed coat. We defined wing length as the distance between the middle of the base chord of the wing to the farthest point on the wing, and its width as the maximum chord length normal to the length of the wing.

We grouped the seeds into three morphotypes based on the ratio of smallest wing area to largest wing area: (1) a functionally "single-winged," (2) "asymmetrical double-winged", and (3) "symmetrical double-winged." The cutoff between the two double-wing morphotypes was made at a smallest/largest wing surface area ratio of 0.75. For geometric morphometrics shape analysis we used TPS suite software (Rohlf, http://life.bio.sunysb.edu/morph) to create a consensus shape of each morphotype based on three single-winged, fifteen asymmetrical double-winged, and five symmetrical double-winged seed types. We selected ten relatively small seeds from a mature kauri cone (*Agathis australis* from the University of California Botanical Garden at Berkeley; specimen number 73.0561) for the same process. The figured seeds are reposited in the Paleobotanical Collections of the University of California Museum of Paleontology (UCMP specimen numbers 254910, 254911, 254912). We chose the seeds of this species because of their similarity to the single-winged seeds of *Manifera talaris*. Depending on the morphotype and taxon, we used 3 or 4 landmarks and 60–135 semi-landmarks to trace the seed outlines and generate the respective consensus shapes (Fig. 3).

Model Construction.—For our experiments, we produced three different seed morphotype models of *Manifera talaris*—single-winged, asymmetrical double-winged, and symmetrical double-winged seeds—each in a range of different weight classes. To validate our methods, we also produced and tested the similarly shaped seeds and models of extant *Agathis australis* (Mirams 1957; Owens et al. 1997).

For the construction of the models, we rescaled the *Manifera talaris* and *Agathis australis* seed consensus shapes to an average

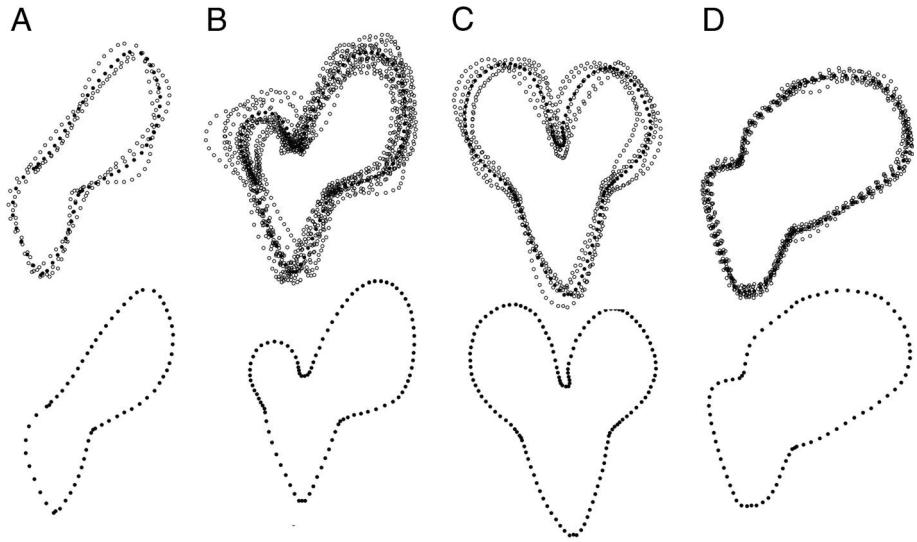

FIGURE 3. (Semi-)landmarks of size-normalized *Manifera talaris* and *Agathis australis* seeds. Original seed shapes (upper row) and resulting consensus shapes (lower row). A, Single-winged *M. talaris*. B, Asymmetrical double-winged *M. talaris*. C, Symmetrical double-winged *M. talaris*. D, Single-winged *A. australis*.

surface area of 0.80–0.82 cm^2 using Adobe Illustrator (CS 6, Adobe Systems Inc.). These scaled vector tracings were used to laser cut (VLS 6.60, Universal Laser Systems, Scottsdale, Arizona) the base shape of the models from tissue paper (Spectra® Deluxe Bleeding Art Tissue™) with an area density similar to that of the wings of *A. australis* (1.75 and 1.80 mg cm^{-2}, respectively) (Supplementary File S3). Whereas the weights of extant *A. australis* seeds are easy to determine, we lack accurate estimates for the fossil *M. talaris* seed weights. Comparison with similar-sized *A. australis* seeds suggests that *M. talaris* seeds may have weighed 6–7 mg. To control total weight, and because seed weight also may reflect a trade-off in parental investment, we varied seed and seed model weights over a wide range (~3.5–15.5 mg) through use of oval-shaped weights cut from an adhesive polyester film (Artist and Craftsman Supply, Berkeley; density 9.86 mg cm^{-2}) (Supplementary File S4). We placed the weights on the seeds' body centroids, parallel to the central axis of the seed body, and weighed each seed and model (Mettler Toledo Mx5, resolution 0.01 mg). Variation in weight was 0.5–2.5 times the mean weight of the *A. australis* seeds from the UCB Botanical Garden (on average 7 mg), or 20–85% of the average reported weight of seeds of this species reported in other studies (i.e., up to 18.5 mg for much larger seeds; Royal Botanic Gardens Kew Seed Information Database 2008).

Experiments.—In order to reconstruct the aerodynamics of the descent of *Manifera talaris* seeds, we used a high-speed camera to examine the flight performance of same-scale models, dropped in a controlled environment. We used two setups: a wider camera view (70 cm away) at lower frame rate was used to establish the frequency of different descent modes, whereas a closer camera view (50 cm away) at a higher frame rate was used to measure detailed autorotation kinematics. Descents of the models and seeds were captured with a high-speed camera (HiSpec 1, Fastec Imaging, San Diego, Calif.) operated at 240 or 500 frames per second and equipped with a 25 mm f/1.4 lens (Navitar, Rochester, N.Y.) (for an example see Supplementary File S5). Lighting was provided by a pair of 150-W flood lamps. Models and seeds were held with forceps at the chalazal end, oriented parallel to the ground, and dropped 2 m above the field of capture via a ladder and a hard-mounted ring used to provide a consistent drop position. A scale, held parallel to the falling seeds' trajectory and at the same distance from

the camera, was visible in every video. The scale and the ring were several diameters of disk area away from the seed flight path to avoid aerodynamic interactions. We dropped the seeds and models in still air, shielded from ventilation within an enclosure purpose-built for studies of directed aerial descent in insects (Zeng 2013) and small vertebrates (Evangelista 2013; Evangelista et al. 2014a).

To examine descent mode, we dropped all seeds and models ten times. In all cases, the filmer noted an initial determination of descent mode. Video was retained for further detailed study for all cases in which the seed remained in focus within the viewing volume. To examine autorotation kinematics, seeds and models were dropped until five autorotational descents were captured in focus and within the viewing volume, or until five consecutive failures to capture such a descent occurred. We recorded a total of 103 specimens (78 models of *M. talaris* in three morphotypes and a range of different weights; ten models of *A. australis* and 16 *A. australis* seeds) in 486 separate videos comprising 100 GB of data.

Digitization and Analysis.—We determined seed position in the videos by manually digitizing two points (distal wing tip, seed body center) using the MTrackJ plugin (Meijering and Smal 2012) for ImageJ (NIH, Bethesda, Md.). All videos in which we observed autorotation were digitized, for a total of 60,176 points. For digitization in each video we used a sequence of frames in which at least two rotations of the seed were in focus and in the middle of the screen away from any barrel distortion and at steady state; for these sequences every frame was digitized. In addition, we partially digitized a reduced set of the descent mode videos to obtain estimates of the descent speed and of the frequency of rotations, for comparison with the autorotation data. We used the scale to convert digitized points to positions.

By using a series of custom-written scripts for Python (version 2.7.3, with Numpy version 1.8.0 and Scipy version 0.9.0) and R (version 3.0.3 [R Development Core Team 2013] with ggplot2 version 0.9.3.1 [Wickham 2009] and dplyr version 0.1.2) we were able to extract kinematics from the digitized points. From every video, we computed the vertical descent speed V, a primary measure of performance, using finite differences and taking the mean for the entire steady-state video. The inverse of the descent speed, $t_D = 1/V$, gave the descent time per meter, which we used in the discussion as an alternate measure of autorotative performance because of its particular ecological relevance as it scales with dispersal potential. In addition, we used a Fast Fourier Transform (FFT; numpy.fft.rfft) to extract the dominant frequency from seed horizontal position. In autorotative descents this corresponded to the first rotational frequency f_{1R}, whereas in other descent modes this corresponded to the frequency of yawing or helical motions. For every digitized frame, we calculated the angle of the seed with respect to the horizontal. The range (max-min) of this angle gave us the coning angle, β, for each video. We then coded the descent modes, kinematics, seed and model geometry information, and masses into a table for further computation and statistical analysis in R.

To facilitate comparison with other published seed and aerodynamic literature, we computed the Reynolds number (Re), a nondimensional quantity that reflects the relative contribution of inertia and viscosity; we also computed the advance ratio, J, used to examine whether the motion is dominated by the vertical descent speed or the autorotation frequency:

$$Re = \frac{Vl}{\nu} \tag{1}$$

$$J = \frac{V}{2lf_{1R}} \tag{2}$$

where l is the span, and $\nu = 15 \times 10^{-6} \mathrm{m}^2\ \mathrm{s}^{-1}$ is the kinematic viscosity of air. For Re ~1000, we expect inertia to dominate the flow. J appears in studies of bird and bat flight, where $J > 7$ typically indicates forward flight, and $J < 5$ indicates hovering; here we take these to indicate whether V or f_{1R} is driving the aerodynamics.

We also computed the Strouhal number, a nondimensional frequency, as $\mathrm{St} = 1/\mathrm{J}$ for comparisons where $f_{1R} = 0$ (e.g., plummeting). For additional comparisons, we computed disk

loading, tip speed, thrust coefficient C_T, and effective drag and lift coefficients, $C_{D,\text{eff}}$ and $C_{L,\text{eff}}$ (using notation from Azuma and Yasuda 1989):

$$\textit{disk loading} = \frac{mg}{S} \tag{3}$$

$$\textit{tip speed} = 2\pi f_{1R} l \tag{4}$$

$$C_T = \frac{mg}{0.5\rho(2\pi f_{1R} l)^2 S} \tag{5}$$

$$C_{D,\text{eff}} = \frac{mg}{0.5\rho V^2 S_W} \tag{6}$$

$$C_{L,\text{eff}} = \frac{mg}{0.5\rho(2\pi f_{1R} l)^2 S_W} = \frac{C_T}{\sigma} \sim C_l \tag{7}$$

where m is the mass, $g = 9.81\ \text{m s}^{-2}$ is the acceleration of gravity, $\rho = 1.2\ \text{kg m}^{-3}$ is the density of air, $S = \pi l^2$ is the disk area, S_W is the wing area, and solidity ratio $\sigma = S_W/S$. The span l was used in disk area calculations because the instantaneous center and radius of rotation were difficult to determine in most videos. For a wing of near-constant cross-section, the effective lift coefficient here scales as the section lift coefficient, providing a means to check the degree to which the camber (the chord-wise curvature of the wing), etc. of our fossil shapes matches those of extant autorotators. Previous studies of autorotating seeds use nondimensional coefficients drawn from studies of propellers (Azuma and Yasuda 1989; Lentink et al. 2009; Norberg 1973; Varshney et al. 2012; Yasuda and Azuma 1997), but we include here an effective drag coefficient based on descent speed V for comparison to drag-based descent seen in pollen and small plumose seeds (Burrows 1975; Greene and Johnson 1990; Greene and Quesada 1992). For seed and model planforms, we also computed shape descriptors typically used in flight biomechanics, including aspect ratio (eq. 8) and second moment of area (eq. 9):

$$AR = \frac{l^2}{S_W} \tag{8}$$

$$I_{ZZ} = \int\int_{wing} (x - x_c)^2 + (y - y_c)^2 dA \tag{9}$$

During the early to middle Permian, air density (~1.4–1.5 kg m^{-3}) and kinematic viscosity most probably were slightly higher than at present because of elevated oxygen content (~1.5 present atmospheric level [PAL]) and CO_2 levels (4–5 PAL [Berner 2009; Bergman et al. 2004; Montañez et al. 2007]). The higher air density would increase the aerodynamic forces (which scale with ρ) by about 25%. This potentially leads to decreasing descent velocities and increasing descent times by 5% and has been proposed to have been a factor in the evolution of flight in insects during the Carboniferous (Dudley 1998; Dudley and Chai 1996; Graham et al. 1995). Because the model tests were in modern atmospheres, all calculations used modern values for density and kinematic viscosity.

Results

Fossil and Extant Seed Morphometrics.—The shape and size of the seed bodies and wings of the three different *Manifera talaris* morphotypes show distinct differences (Table 1, Fig. 1). On average, asymmetrical double-winged seeds have a larger total area (1.15 cm^2) than the symmetrical double-winged and single-winged morphotypes (respectively 0.83 and

TABLE 1. *Manifera talaris* seed morphotypes and *Agathis australis* seeds.

	Seed body area, cm^2	Total wing area, cm^2	Total seed area, cm^2	% Total wing area of total area
M. talaris symmetric double-winged	0.28	0.55	0.83	66
M. talaris asymmetric double-winged	0.35	0.80	1.15	69
M. talaris single-winged	0.33	0.66	0.99	67
Agathis australis	0.27	0.63	0.90	70

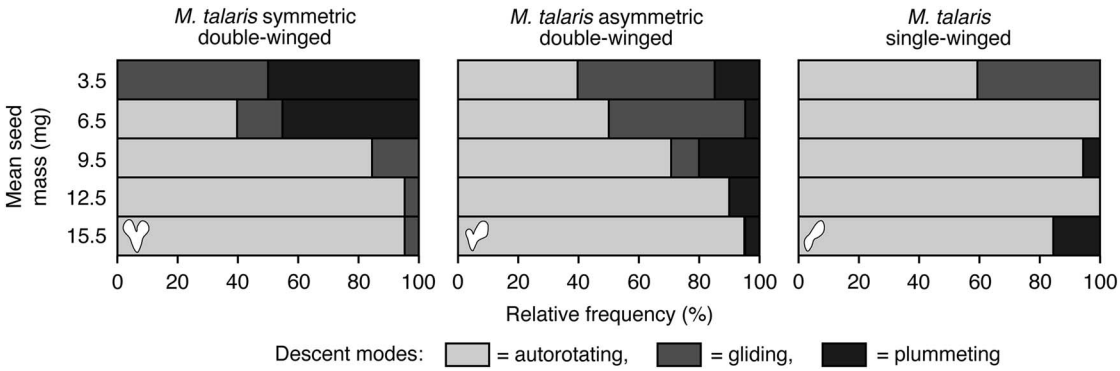

FIGURE 4. Relative descent mode frequencies per mass bin of falling *Manifera talaris* morphotype models.

0.99 cm^2). Seed body geometries are similar in all types, but the symmetrical double-winged seed bodies are 15–20% smaller than the two other types. Wing geometries differ among all three types. Functionally single-winged seeds have long, oblong primary wings that are the longest of all the morphotypes and a secondary wing that is reduced to such an extent that it is rudimentary. Asymmetrical double-winged seeds have trapezoidal to obovate primary wings that are somewhat shorter, but the increased flaring on the lower edge of the wing results in an average area that is comparable to that of the single-winged morphotype. The secondary wing of the asymmetrical double-winged seeds is similar in shape to the obovate-to-oval wings of the symmetrical double-winged seeds. They are, however, reduced in size such that they make up less than 35% of total wing area in all samples. Both wings of the symmetrical double-winged seeds are roughly similar in size and shape. Despite the differences in wing size and morphology, the average total wing area as a proportion of the average total area differs by only 3% among the morphotypes (range of 66–69%). To maintain similar surface areas across the models of all three seed morphologies, we scaled the single-winged and asymmetrical double-winged models to 82% and 70% the size their fossil counterparts, respectively. This allowed us to compare the effect of seed shape on flight performance and kinematics independent of seed size.

Seed bodies of *Agathis australis* are comparable in size to *Manifera talaris*'s symmetrical double-winged morphotype (~0.28 cm^2; Table 1). The oblong wing of *A. australis* is shorter than the primary wing of both the single- and the asymmetrical double-winged *M. talaris* morphotypes, but its consistent width results in an area that is similar to both. The average total wing area as a proportion of the average total area is 70%, similar to that of the fossils. The seed body accounts for approximately 80% of the total weight of the seed.

Assuming the center of rotation in autorotative descent is approximately in the center of the seeds, the average seed lengths would give a maximum disk area approximation of 10.9 cm^2, 7.48 cm^2, 6.11 cm^2, and 6.92 cm^2 for the single, asymmetrical and symmetrical double-winged *Manifera talaris* models and *Agathis australis* seeds, respectively. The average maximum chord length of the single-winged seeds is a quarter smaller than that of the larger wing of the asymmetrical double-winged types (0.63 cm vs. 0.8 cm, respectively), but longer than that of the symmetrical double-winged seeds (0.56 and 0.55 cm). The difference in lengths and widths of the single-winged seeds and the larger wing of asymmetrical double-winged seeds results in wing areas that are approximately the same (0.66 cm^2 vs. 0.65 cm^2 respectively). In order to compare the effect of the different seed morphologies in the experiments, we rescaled their consensus shapes so that they had a constant area. See Table 2 for the geometric properties of the *A. australis* seeds and rescaled models.

Descent Mode and Frequency.—Figure 2A–D illustrates representative descents for all

TABLE 2. *Manifera talaris* and *Agathis australis* seed and models geometric properties for aerodynamic calculations and comparisons. Ranges given indicate the minimum and maximum values. Seed consensus shapes depicted in Figure 3. To provide equal-area comparisons, models were scaled to have constant area of about 0.8 cm^2.

	Manifera talaris models			*Agathis australis*		
	Symmetric double-winged	Asymmetric double-winged	Single-winged	Model	Seed	Other comparisons
Mass, $\times 10^{-6}$ kg	3.25–15.9	3.25–15.5	3.46–15.7	6.56–15.19	5.64–15.56	13–58 *Acer*[1] 23 *Pinus*[1] 58 *Fraxinus*[1] 12.9 *F. griffithii*[2] 50 *Liriodendron*[1] 7.5 *Picea*[3]
Wing area, S_W, $\times 10^{-4}$ m^2	0.794	0.827	0.830	0.899	0.981	0.56–3.04 *Acer*[1] 1.09 *Pinus*[1] 0.615 *F. griffithii*[2]
Span, *l*, cm	1.4	1.5	1.9	1.5	1.5	1.48–3.62 *Acer*[1] 2.19 *Pinus*[1] 2.4 *F. grifithii*[2] 1.4 *Picea*[3]
Disk area, *S*, cm^2	6.11	7.48	10.9	7.04	6.92	4.49–25.5 *Acer*[1] 10.1 *Pinus*[1]
Solidity ratio, σ, %	13	11	7.6	13	14	12 *Acer*[1] 11 *Pinus*[1] 7.4 *F. griffithii*[2] 13 *Picea*[3]
Aspect ratio, *AR*	2.4	2.9	4.2	2.5	2.2	3.83–4.33 *Acer*[1] 4.43 *Pinus*[1]
Mean chord, cm	0.56	0.54	0.44	0.60	0.66	0.38–0.84 *Acer*[1] 0.50 *Pinus*[1]
Wing loading, N/m^2	0.4–2.0	0.4–1.8	0.4–1.9	0.7–1.7	0.6–1.6	1.87–2.24 *Acer*[1] 2.05 *Pinus*[1] 2.12 *F. griffithii*[2] 1.63 *Picea*[3]
Disk loading, N/m^2	0.05–0.26	0.04–0.24	0.03–0.14	0.09–0.21	0.08–0.22	0.22–0.29 *Acer*[1] 0.22 *Pinus*[1] 0.16 *F. griffithii*[2] 0.21 *Picea*[3]
Second moment of area, $I_{ZZ} \times 10^{-9}$ m^4	1.286	1.502	2.071	1.683		

Sources: [1]Table 1 of Azuma and Yasuda 1989; [2]Table 4 of Minami and Azuma 2003; [3]Norberg 1973.

observed modes: plummeting, gliding with a constant yaw turn, autorotation, and autorotation with sideslip. All morphotypes exhibited these modes, but the relative frequencies of each varied substantially between morphotypes (Fig. 4). In the lower weight classes (3.5–9.5 mg) the double-winged morphotypes failed to initiate autorotation in more than half of the cases, resulting in a plummeting or gliding descent. In all the weight classes combined, autorotation was the most frequently observed descent mode for the single-winged morphotype. We did not observe straight-like stable glides, parachuting stable drag descents, or rolling autorotation about the long axis in either *Manifera talaris* or *Agathis australis*.

Flight Performance, Aerodynamic Parameters, and Autorotation Kinematics.—For a quantitative biomechanical comparison of falling-seed models used in our experiment and in similar studies in the literature, we have included a wide range of commonly assessed parameters and measurements related to flight performance: Table 2 compares wing geometries for the models and several extant autorotating seeds

TABLE 3. *Manifera talaris* and *Agathis australis* seed and models aerodynamic properties and comparisons. Values show mean ± SD and include all weight classes tested. For more detailed information see supplementary Figures 5 and S1. The variation in parameters reflects the intentional changing of model weights in the range 3.5–15 mg.

	Manifera talaris models					
	Symmetric double-winged	Asymmetric double-winged	Single-winged	*Agathis australis* Model	*Agathis australis* Seed	Other comparisons
Autorotation frequency, f_{1R}, Hz	16.3 ± 4.0	20.8 ± 7.2	21.8 ± 7.3	22.8 ± 8.3	23.9 ± 7.9	16–30 *Acer*[1] 24 *Pinus*[1] 19 *F. griffithii*[2] 20 *Picea*[3]
Rate of descent, V, m s^{-1}	1.41 ± 0.44	1.06 ± 0.35	0.83 ± 0.21	0.83 ± 0.13	0.78 ± 0.15	0.8–1.1 *Acer*[1] 1.0 *Pinus*[1] 1.1 *F. griffithii*[2] 0.64 *Picea*[3]
Coning angle, β, deg	39 ± 11	31 ± 18	20 ± 17	16 ± 11	17 ± 7	15–27 *Acer*[1] 21 *Pinus*[1] 22 *Picea*[3]
Thrust coefficient, C_T	0.13 ± 0.05	0.06 ± 0.03	0.03 ± 0.03	0.06 ± 0.03	0.05 ± 0.02	0.03–0.05 *Acer*[1] 0.02 *Pinus*[1]
Reynolds number, Re	1313 ± 410	1095 ± 355	1028 ± 265	832 ± 131	768 ± 149	500–1370 *Acer* 750 *Pinus*[1]
Tip speed, m s^{-1}	1.43 + 0.35	2.01 ± 0.69	2.45 ± 0.85	2.14 ± 0.78	2.23 ± 0.74	2.3–2.4 *Acer*[1] 2.75 *Pinus*[1]
Tip speed ratio	1.1 ± 0.3	2.0 ± 0.8	3.1 ± 0.1	2.7 ± 0.7	2.8 ± 0.5	0.3–0.5 *Acer*[1] 0.36 *Pinus*[1]
C_T/σ	1.0 ± 0.4	0.5 ± 0.3	0.4 ± 0.4	0.5 ± 0.2	0.3 ± 0.1	0.2–0.4 *Acer*[1] 0.2 *Pinus*[1]

Sources: [1]Table 2 of Azuma and Yasuda 1989; [2]Table 4 of Minami and Azuma 2003; [3]Norberg 1973.

(including equations 9–10). Table 3 compares the resulting autorotation kinematics and nondimensional aerodynamic parameters for these same seeds. Autorotation kinematics are summarized in Figure 5, which shows the effect of seed mass on coning angle, autorotation frequency, and vertical descent speed. Modes and nondimensional aerodynamic parameters (eqs. 1–8) are shown in Figure 6 and Supplementary Figure S1. Descent time (s/m) at terminal velocity is shown in Figure 7.

In general, overall flight performance improved in going from double-winged symmetric, via double-winged asymmetric, to single-winged morphotypes. Furthermore, whereas increases in mass might be expected a priori to increase the descent speed for a case of simple drag ($v \sim m^{0.5}$), this appears not to be the case during autorotation. As mass increased, the coning angle decreased and rotational frequency increased in ways that kept changes in descent speed (Figs. 5 and S1) and descent time (Fig. 7) unexpectedly small.

Biomechanical Evaluation

Model Validation.—Obviously, the terminal velocity of shed conifer seeds in the Paleozoic cannot be directly measured from fossils. Evaluating the performance of the range of seed morphologies produced by *Manifera talaris* called for an empirical approach using seed models. In the same-scale model experiments we tested the validity of our models by comparing flight characteristics of similarly made seed models of the extant *Agathis australis* with the real seeds the models were based on. Overall flight performance was similar between model and actual *Agathis australis* seeds (Fig. 7). As mass was varied, the observed autorotation kinematics (Fig. 5, right two columns) and nondimensional parameters (Fig. S1) were identical for model and actual seeds of *A. australis*. In addition, all observations fell within the ranges reported by others for extant autorotating seeds of similar mass (Tables 2, 3). This suggests that

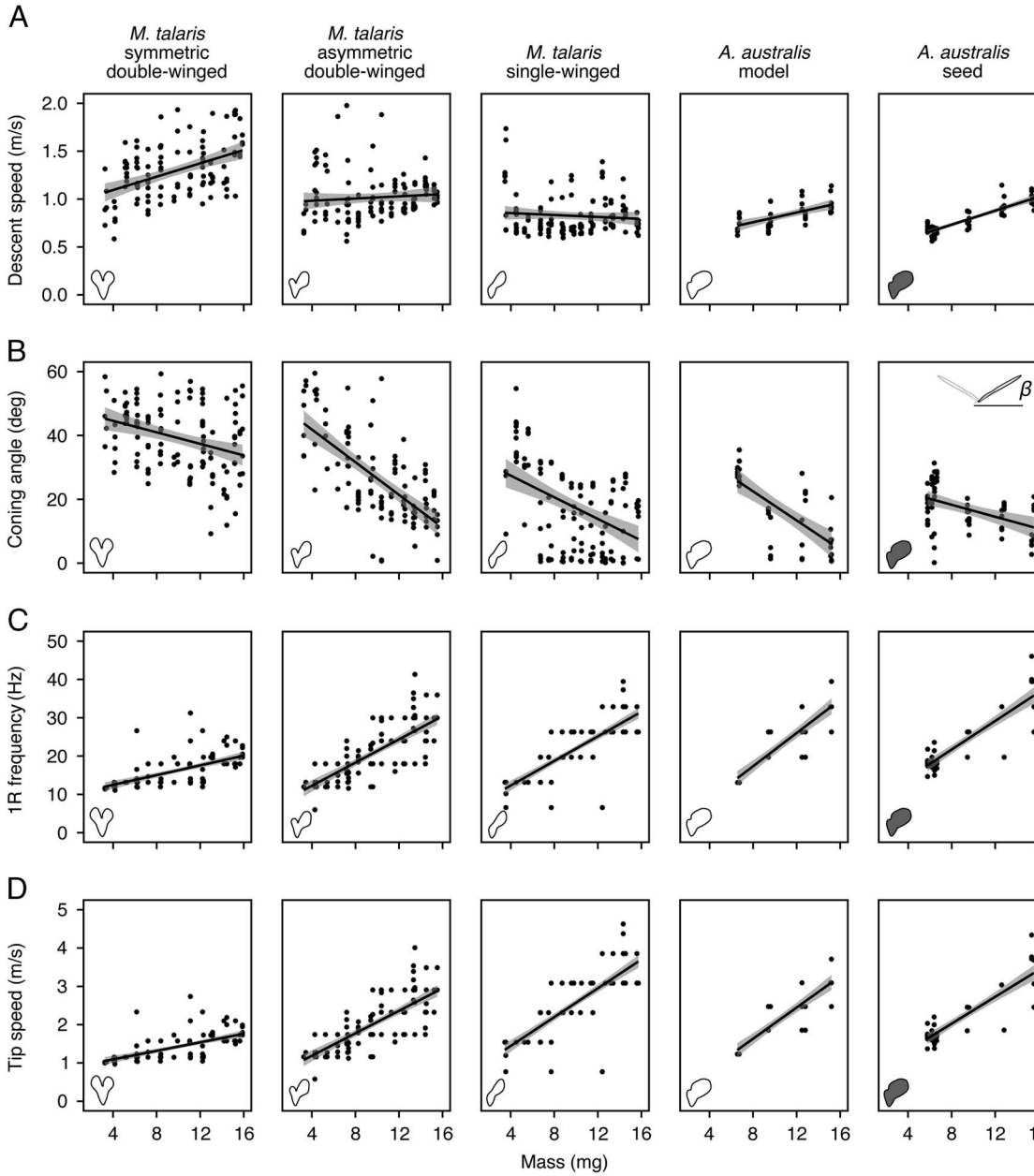

FIGURE 5. Autorotation kinematics with increasing mass. All parameters are plotted against mass (mg) of *Manifera talaris* models and *Agathis australis* models and seeds. A, Descent speed (V, m/s). B, Coning angle (β, deg, see inset detail). C, Autorotation frequency (f_{1R}, Hz). D, Tip speed (eq. 4, m/s).

our same-scale model approach provided a realistic reconstruction of the flight performance of the seed of *M. talaris*.

Reconstructed Flight Performance.—As expected, the aerodynamic characteristics of the various seed morphologies produced by *Manifera talaris* were quite different. The model study yielded three important observations for the three contrasting morphologies in *M. talaris*:

1. Initiation of autorotation failed frequently in symmetrical double-winged seeds, less frequently in asymmetrical double-winged seeds, and infrequently in single-winged

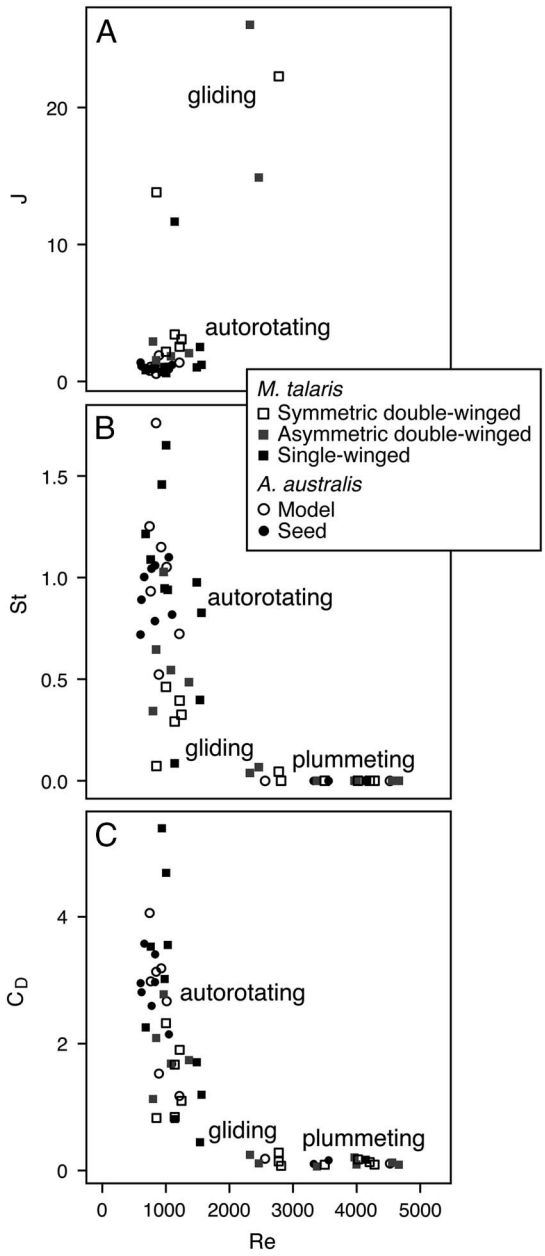

FIGURE 6. Nondimensional aerodynamic parameters and descent mode in *Manifera talaris* models and *Agathis australis* models and seeds. A, Advance ratio (*J*, eq. 2). B, Strouhal number (*St = 1/J*). C, Drag coefficient ($C_{D,eff}$, eq. 6). All plotted against Reynolds number (Re, eq. 1). Autorotation takes place at low advance ratio and high effective drag; gliding and plummeting are characterized by very high advance ratio and low effective drag. For all modes, Re ~ 1000.

seeds. Failed initiation of autorotation resulted in plummeting or gliding. Failing autorotation was most frequent in the lighter seeds.

2. Even during autorotative flight, the symmetrical double-winged seeds descended much faster on average (1.3–1.7x) than the other morphologies.
3. As symmetrical double-winged seeds increase in weight, their median descent velocity roughly increased with the square root of their weight (as predicted by scaling), even when autorotating. In contrast, the terminal descent velocity of their single-winged and asymmetrical double-winged counterparts hardly changed with increased wing loading, ranging from 6 to 29 mg/cm^2. Hence, flight effectiveness during autorotation actually increased with wing loading; single-wing and asymmetrical double-winged autorotators would have been able to transport larger seeds without compromising descent performance.

Flight Kinematics as Mass and Disk Loading Change.—As mass is increased within an asymmetrical double-winged or single-winged morphotype, the vertical speed and descent times can be held within a relatively constant and useful range. The changes in autorotation flight kinematics as mass changes can be understood from a free body diagram (Fig. S2, after Burrows 1975; Norberg 1973). For an asymmetric wing with the weight of the seed placed nearest the chalazal end, the aerodynamic forces on the wing act at a point different from the center of mass. During autorotation, the seed must be inclined at some coning angle, and must be spinning, so that the vertical component of the aerodynamic forces (lift and drag) balance the weight, while the horizontal component results in the centripetal acceleration for spinning (Fig. S2A). As mass increases, reduced coning angles (Fig. 5B) balance the added weight by providing a larger vertical component of the resultant aerodynamic forces (Fig. S2B). This confirms observations in other studies of extant autorotators (Norberg 1973; Azuma and Okuno 1987). Aerodynamic forces scale as the square of speed, so as mass increases, speeds should increase. In autorotation, as loading increases, both autorotational frequency (f_{1R}) and vertical speed (V) increase (Fig. 5A,C).

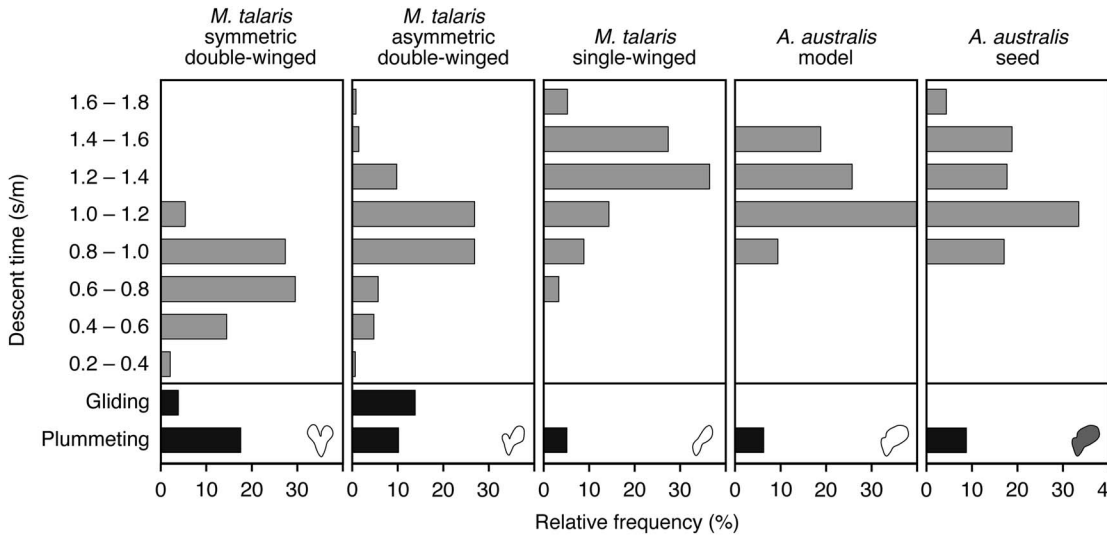

FIGURE 7. Wind dispersal potential. Summary diagram, combining results from the descent mode and aerodynamics experiments with *Manifera talaris* models and *Agathis australis* models and seeds, showing the relative frequency of seeds and models that plummet and glide (black bars), and autorotate with various levels of effectiveness (i.e., descent time bins at terminal velocity; gray bars). Each frequency distribution is the average of the frequency distributions of four discrete mass intervals of seeds and models: 5–8, 8–11, 11–14, and 14–17 mg. Results of even lighter models (<5 mg; shown in, for instance, Figs. 4 and 5) were not included because such small masses were not encountered in the *A. australis* seeds.

For single-winged *Manifera talaris* seed models, however, the increase in autorotational frequency is enough to increase lift to such an extent that vertical speed hardly changes despite a quadrupling of mass (Fig. 5A). This outcome also matches the results of Norberg (1973) and Azuma and Okuno (1989) and the trends correspond to what Varshney et al. (2012) observed when they sequentially trimmed away the wings of *Acer* samaras.

Because of the changes in coning angle and autorotation frequency, vertical speed during autorotation is relatively insensitive to seed mass in single-winged or asymmetrical double-winged *Manifera talaris* and *Agathis australis*. If we consider seed mass as a measure of parental investment, the ability to increase the seed mass with somewhat constant transport costs (same size and mass of wing) would be advantageous whenever long-distance dispersal improves a population's fitness. A biomechanical limit to this could be the seed weight at which it can no longer set up stable autorotation. Experiments with non-biological cut cards and balsa models to probe this limit did not identify a weight limit (Yasuda and Azuma 1997) and neither did the trimming of wings of diaspores in *Acer* (Varshney et al. 2012). Nor did the variation in weights—50% to 250% of extant *A. australis* of similar area and linear dimensions—used here. However, drop studies comparing multiple species suggest mass scaling eventually catches up (Greene and Johnson 1993).

Biomechanics of Manifera talaris Seeds and Extant Gliders and Autorotators.—Our estimated *Manifera talaris* descent speeds, autorotation frequencies, and nondimensional coefficients are about the same as for previous studies of extant autorotating seeds (Azuma and Yasuda 1989; Minami and Azuma 2003; Norberg 1973; Nathan et al. 2002) (Tables 2, 3), as well as for our models versus actual seeds of *A. australis* (Figs. 5 and S1). This suggests that our modeling approach is valid. The thrust coefficient (Table 3) and effective lift coefficients (Fig. S1C) match extant examples, suggesting there are no unmodeled camber or wing-section effects in our physical model. Although the cross-section of the seed may be difficult to observe in compression fossils, the coefficients would suggest that details of

the wing section do not substantially drive the autorotative performance seen here.

In 486 trials, the seeds never went into the rolling autorotation modes as described, for instance, for *Eucommia* (Call and Dilcher 1997) or for the tulip poplar, *Liriodendron tulipifera* (McCutchen 1977). We also did not observe Magnus-effect rotational lift in *Manifera talaris* or *Agathis australis*. The seeds and models were too heavy for drag-based "parachuting" modes seen only in very light, plumed or pappose seeds (Greene and Johnson 1990; Greene and Quesada 1992; Minami and Azuma 2003). Long-distance straight-line stable glides as in *Alsomitra macrocarpa* (Azuma and Okuno 1987) or other straight gliders also were not observed (Burrows 1975; Minami and Azuma 2003). We propose that the absence of straight-line glides is due to asymmetry and instability (Varshney et al. 2012; Evangelista 2013; Evangelista et al. 2014a,b). Distinct modes, with wide separation between the nondimensional aerodynamic parameters, occur because of mechanical bifurcations; i.e., small amounts of asymmetry result in instability that mechanically enforces differences in kinematics and aerodynamics and thus results in a different descent mode. In the seeds discussed here, straight-line gliding appears to require more precise control of symmetry than other modes; a small degree of asymmetry will result in turning or spinning behavior that pushes the diaspore into autorotation. This difference in sensitivity to small variations in morphology among descent modes may offer a mechanical explanation for why some modes appear more frequently in the plant world than others.

In *Manifera talaris* and *Agathis australis*, seeds were observed to plummet, stably glide in a helical pattern at high advance ratio, and autorotate at low advance ratio (Figs. 2, 6). The first mode, plummeting, happens for a heavy seed with no wing or a very small wing in relation to its weight. Plummeting is not very useful for dispersal but should be considered a reasonable assumption for an ancestral condition. As wing surfaces became more elaborate, they would have been symmetric or asymmetric. Symmetric wings appear to do best if they have a large area and glide stably, either in a classic stable glide as in *Alsomitra macrocarpa*, through use of phugoid mode, or through use of rolling Magnus-effect mode as in some *Liriodendron tulipifera* (some tulip poplar seeds have marked asymmetry; these combine rolling and autorotation). There are two constraints. First, to achieve stability, the shape of the seed must be close to symmetric (as seen in the examples of Minami and Azuma 2003). Empirically, even the slight left-right difference in our symmetrical double-winged *M. talaris* models appears enough to prevent long- distance straight-line glides (see below). Nor do our seeds have strong differences in the inertias about the principal axes (Varshney et al. 2012) that would stably sustain rolling autorotation. The second constraint is that the static stability achievable by a flying-wing seed is limited to the moments that can be generated as the center of pressure moves forward or aft a few percent of the chord (short direction along the wing). This may limit static-stability gliding to low-wind, low-turbulence situations. Such conditions are common for the environments in which *A. macrocarpa* grows. This species, a liana from Malaysian and Indonesian rain forests, produces diaspores with large thin wings that are well known for their stable glide (Azuma and Okuno 1987), but the *Alsomitra*-type winged seed is not widely distributed in regions with higher wind or turbulence.

A winged seed with even moderate asymmetry should result in two types of descent. During stable glides, the asymmetry will result in flight paths with slight, constant yaw, wasting a portion of lift on side forces, and reducing the probability of very long, straight-line glides. The helical path expected in this condition is seen in the lower weight classes of both model *Manifera talaris* and *Agathis australis* seeds and their models. As wing shapes (or the mass loading) become even more asymmetric, they are forced into autorotation, in which large effective drag coefficients are achievable owing to the squared dependence of forces on autorotation frequency. This is seen empirically here as shape changes from double-winged symmetric through double-winged asymmetric and single-winged, and also when wing loading is changed by increasing the mass of the off-center ballast of the seed

(Fig. 5, Supplemental Fig. S1). During autorotation, the offset between the center of mass and the net aerodynamic center as the wing spins means that restoring moments scale with the span of the wing, making it potentially more stable than could be achieved in straight-line stable gliding. Stabilization in this manner is also seen in extant angiosperm autorotators, e.g., *Buckleya joan* and *Tilia miqueliana* (Azuma and Yasuda 1989), and in the much smaller "parachuting" seeds like *Taraxacum* (Greene and Johnson 1990). Aside from the mass distribution (Yasuda and Azuma 1997), countertorques generated by spinning also would stabilize the rotation (Hedrick et al. 2009; Varshney et al. 2012). This is important in the face of environmental disturbances: if the parent trees are canopy trees or lianas, or stand in relatively open stands, this allows the seed to exploit higher winds (Horn et al. 2001; McCay 2003). Morphologies that remain stable in turbulence (Childress et al. 2006; Evangelista 2013; Evangelista et al. 2014b) could use this property to remain aloft or to enhance dispersal, by continuing to function when the possibility of large gusts is higher. In our results, autorotating seeds were able to maintain stability even with large horizontal translational velocities superimposed on top of the descent. Of autorotating descents, 18% had a measurable sideslip, and in a few extraordinary trials, stable sideslip velocities ranged as high as 0.96 m s^{-1}, up to 80% of the descent speed.

Autorotation generates large forces by virtue of fast relative motion between the wing and the air, parallel to what is seen in animal flight (Norberg 1973; Dudley et al. 2007; Evangelista 2013; Evangelista et al. 2014a). Another mode of decent that might be predicted is the use of the broad surface of the diaspore as a "parachute". However, even if *Manifera talaris* were to retard its descent using the maximally achievable bluff body parachuting drag, it would fall 1.4 to 2.2-times faster ($v = (2mg/\rho AC_D)^{-2}$) than the autorotating case. The high drag parachuting strategy only works for small and tiny seeds that are able to exploit high drag at much lower Re (for Re <1, drag coefficients scale inversely with Re); these seeds experience Re ~1000. A large high-drag surface would be subject to premature detachment (Schippers and Jongejans 2005; Evangelista et al. 2011) in low winds, disadvantageous for the dispersal of viable offspring. The compressed form seen in all *M. talaris* morphotypes would be unstable during parachuting, and thus unable to function in high winds or high turbulence that, in the autorotation case, could carry seeds on occasional long-distance dispersal paths (Hughes et al. 1994; Clark 1998; Nathan et al. 2008).

Paleoecological and Evolutionary Discussion

Ecological and Biogeographical Implications.—The ecological implications of the autorotative seed dispersal syndrome have been discussed in several studies (Green 1980; Augspurger 1986; Greene and Johnson 1989, 1992; Horn 2001). The ecological relevance of slowing down seed descent lies in the modification of seed dispersal patterns. For wind-dispersed seeds, the strongest predictor for dispersal distance is horizontal wind speed (Nathan et al. 2001). After that, seed release thresholds, release height, terminal velocity of the seed, and canopy structure are the most important factors (Okubo and Levin 1989; Nathan et al. 2001; Levin et al. 2003; Schippers and Jongejans 2005). In order to make the most of horizontal winds, seeds have to maximize their flight time, which is a function of release height and descent velocity (Fig. 7). Maximization of descent time in a manner that is stable in turbulent, gusty wind conditions is especially advantageous for long-distance dispersal. Seeds with a morphology that makes them effective autorotators, rather than gliders or plummeters, do exactly that: they excel in longer mean descent times (Fig. 7) because aerodynamic stability allows them to keep going even when perturbed by gusts. This has profound effects on their potential dispersal distance and the geographical shape of the dispersed seed distribution. Furthermore, seeds that autorotate like *Manifera talaris* or *Majonica alpina*, growing on relatively small dwarf shoots with their large wings sticking out, likely have a larger chance of becoming dislodged as a result of gusty winds than simple wingless seeds would have. Thus, the

moment of release of autorotative seeds would have had an enhanced chance of coinciding with the very conditions (horizontal and turbulent winds) they optimally exploited.

Most studies on the dispersal of autorotating seeds show a unimodal leptokurtic distribution surface, with a sharp peak close to the parent plant, and more distally a long tail (Levin et al. 2003). The differential flight characteristics of the various seed morphologies produced by *Manifera talaris* would have added even more kurtosis to its seed distribution compared with the distributions of extant autorotating conifers, making the distribution pattern hyperleptokurtic. The plummeting (a)symmetrical double-winged seeds add to the "peakedness" in seed frequency near the parent plant, whereas the (almost) single-winged autorotators make for a longer tail, yet one that is thinner than in obligate autorotators, since only a portion of all the *Manifera* seeds have these flight capabilities. The long tail would result in occasional dispersal events of extremely long range, thus having a disproportionately large effect on seed-shadow size.

In 2004, Howe and Miriti listed three reasons why it may be important for seedlings that their parent plant have effective seed dispersal mechanisms: (1) to escape density-dependent mortality near the parent plant; (2) to colonize open habitats; (3) to travel to microsites required for establishment (based on Howe and Smallwood 1982). An increase in seed dispersal potential will affect the speed with which plant populations can shift their range during rapid climate change (e.g., Clark 1998; Nathan et al. 2002; Soons and Bullock 2008), but also change their spatial and genetic heterogeneity. Therefore, we propose two more situations in which greater dispersal potential is important, especially on slightly longer time scales: (4) when a species living in scattered habitats of an ephemeral nature (e.g., wetlands) must escape the old locality as it disappears, and find and colonize new habitats; and (5) when migration speed is of the essence, e.g., during times of rapid climate change and the resulting fast latitudinal shift of biomes.

The last two situations, a need to find ephemeral, scattered habitats and a need for high migration rates, might have been important for early to middle Permian Euramerican plant populations. During this time period the equatorial Euramerican floral realm became increasingly arid (or rather, less wet) as a result of changes in volume of the Southern Hemisphere ice caps (Montañez et al. 2007). Initially, during the very beginning of the Permian, merely seasonally dry habitats extended over large, interconnected parts of the landscape, whereas the dryer "seasonally wet" habitats may have coexisted in smaller isolated patches (DiMichele et al. 2006). As dry seasons became progressively longer, a gradual change in the structure of the habitat landscape took place. The seasonally wet patches increased in size and started to connect, whereas the wetter seasonally dry habitats were shrinking and became fragmented. Aridification, however, progressed even further and by the end of the early Permian, seasonally wet habitats also shrank and fragmented, and corridors flanking river channels were probably among the few environments that supported rich plant life in the Midland Basin (DiMichele et al. 2006).

The Lower Pease River flora is one of only two fossil floras known from the Midland Basin from this particular time interval (DiMichele et al. 2001, 2004). The fossil flora is dominated by relatively drought-tolerant seed plants such as the voltzian conifers *Manifera talaris* and *Lebowskia grandifolia*, ginkgophytes, and cycadophytes. The assemblages are para-autochthonous and thus represent local plant communities growing near the small channels in which they were deposited and preserved. Paleosols and sedimentary patterns indicate that the environments these plants grew in were predominantly hot and dry, with a short rainy season (DiMichele et al. 2006). The Lower Pease River flora represents a species pool distinct from the preceding Clear Fork floras (Chaney and DiMichele 2007). The Lower Pease River Flora likely migrated in from somewhere else in the region, perhaps from areas where orographic rainfall might have differentiated this flora from that of the basinal lowlands. Winged seeds may have enabled increased migration speeds for *M. talaris* during the expansion phase of the early Permian seasonally wet areas, and increased the chances of reaching

new habitats when habitable areas became limited and scattered over the landscape.

Evolutionary Implications.—In order for their populations to maintain a high fitness, extant plant lineages adhering to various ecological strategies rely on efficient long-distance seed dispersal. Thus, it seems reasonable to assume that in the past various seed morphologies that facilitated more efficient long-range dispersal produced peaks in the fitness landscape of their producers. Accordingly, extant plants display a wide range of seed dispersal mechanisms, such as co-option of small-sized animal hosts, direct dispersal using dehiscent mechanisms, and wind dispersal utilizing drag, lift, combinations of these, or autorotation (e.g., Van der Pijl 1982; Tiffney and Mazer 1995; Willson and Traveset 2000). Although the morphology and function of the autorotating voltzian conifer seeds are comparable to extant ones, the ecosystems in which they evolved were certainly not. Seed predation and dispersal by arthropods and vertebrates did not become prevalent until the Mesozoic (Tiffney 1986, 2004; Labandeira 2002; Leslie 2011). In the absence of suitable animal vectors for seed dispersal in the Paleozoic, adaptive opportunity to improve dispersal was rather limited. Water-bound plants may have developed more-effective hydrochorous diaspore dispersal syndromes (e.g., *Lepidophloios*'s aquacarps [Phillips and DiMichele 1992]), but for Paleozoic plants with non-hydrophytic, non-riparian lifestyles wind dispersal was the only long-range option.

The benefits of more effective wind dispersal include an increased seed-shadow size, and broader seed-shadow frequency distribution with a long tail, indicating still rare, but relatively more frequent very long-distance dispersal events. These effects allow subsequent generations to colonize new areas away from parental competition and shading, far from established populations of pathogens and the few existing predators (e.g., Nathan and Muller-Landau 2000). Greater seed-shadow sizes and higher frequencies of very long-distance dispersal can also be achieved via production of more seeds, but this would mean a vastly expanded resource investment, as it would mainly result in higher seed densities close to the parent plant. By comparison, the enhanced dispersal performance of autorotating seeds comes at virtually no extra cost; the size investment per seed can even be increased in autorotating seeds at no cost to descent time, further enhancing successful seedling establishment. Moreover, autorotation would have allowed for adaptive flexibility in seed mass with hardly any effect on wind dispersal capability. The evolution of winged seeds in the voltzian conifers would have augmented the fitness of the populations that produced them by speeding up maximum migration rates and permitting the propagules to reach favorable microhabitats, potentially leading to attainment or maintenance of dominance within the plant community.

Winged seeds and diaspores like the ones described here seem to have evolved multiple times and independently in various conifer (Pinaceae, Cupressaceae and Araucariaceae) and numerous angiosperm lineages (e.g., Givnish 1980; Azuma and Yasuda 1989; Farjon 1990, 2005, 2010; Benkman 1995; Schulz et al. 2005; Eckenwalder 2009; Leslie et al. 2013). In extant conifer taxa, symmetric double-winged seeds occur very rarely in *Agathis* species such as *A. robusta* and *A. australis* (Mirams 1957; Kvaček 2002; personal observation). These double-winged seeds are vastly outnumbered by single-winged seeds produced on the same individual plant. The near absence of modern double-winged seeds in *Agathis*, and complete absence in other autorotating seed producing taxa, corroborates the conclusion that the more effectively dispersing single-winged morphology improves the fitness of their producers in the context of their ecological strategy.

An Imperfect Evolutionary Takeoff.—Looy and Stevenson (2014) proposed that the lateral sporophylls of the dwarf shoot may have been predominantly responsible for the production of very asymmetric wing topologies, whereas the central sporophylls primarily produced more bilaterally symmetric ones. Moreover, they found only "left-winged" seeds on the left lateral sporophylls, whereas the right lateral sporophylls bore only "right-winged" single-winged seeds (see Fig. 8A). The only attached seed they observed with a sizable second wing was attached to a median sporophyll. For every

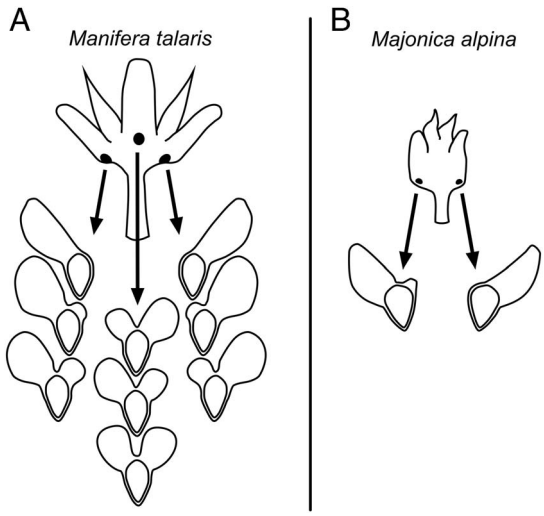

FIGURE 8. Ovuliferous dwarf shoots, sporophyll position, and seed wing morphology. A, Ovuliferous dwarf shoot of *Manifera talaris* and the expected range of seed morphologies produced by the two lateral and one median sporophylls (based on fossil observations, see Looy and Stevenson 2014). B, Typical *Majonica alpina* dwarf shoot lacking a median sporophyll and the seed morphologies it produced (Clement-Westerhof 1987).

median sporophyll there are two lateral ones, which could explain the approximately 2:1 ratio of (almost) single-winged seeds over (almost) symmetrical ones, as observed among 71 dispersed seed fossils collected at the Buzzard Peak locality in Texas (Looy and Stevenson 2014). The oldest conifer known to produce single-winged seeds only (or seeds with a very rudimentary second wing at most) is the late Permian fellow-majonicacean *Majonica alpina* (Clement-Westerhof 1987). Interestingly, almost all its fossilized dwarf shoots lack a median sporophyll (Fig. 8B).

On the basis of our observations of seed morphology and the position on dwarf shoots of *Manifera talaris* and *Majonica alpina*, we hypothesize that the evolution of the autorotative seed dispersal syndrome was a discretely three-stepped evolutionary developmental process within this lineage:

1. Development of lateral integument outgrowths, giving rise to wings that increase chances of wind dispersal when the seed is released or when it is already on the ground.
2. Capacity for overdevelopment of the integument outgrowth at the chalazal end, on the side farthest from the dwarf shoot axis, thus producing a range in wing topologies as observed in *Manifera talaris*, depending on the position of the sporophyll on the dwarf shoot. Because this range includes the autorotative morphologies of superior functionality (in terms of wind dispersal potential), *M. talaris* benefited from greatly improved dispersal capacity and an increase in fitness at little extra cost.
3. Loss of the median sporophyll in winged-seed-producing voltzians (as observed in *Majonica alpina*); thus, an individual's seed production investment is focused on production of the more functional single-winged autorotators only.

Because steps 2 and 3 would have required different types of genotypic adaptation, this hypothesis could explain how *Manifera talaris* may have persisted to produce the full range of seed morphologies, while only a portion of the seeds would have had the high dispersal capability. It is possible that step 3, the loss of the median sporophyll, was induced by developmental adaptations other than, or in addition to, the benefits of more effective seed dispersal. Within the Permian voltzian conifers there is a range in female cone structure from very open dwarf shoot- and bract-bearing fertile zones or shoots, as in *Manifera*'s contemporary *Lebowskia grandifolia* (Looy 2007), to condensed cones with tightly packed dwarf shoots, as in the end-Permian *Pseudovoltzia liebeana* (e.g., Uhl 2004). An evolutionary trend toward more-condensed, better-protected cone-like structures may also have led to reduction of dwarf shoot complexity and loss of sporophylls.

In the fossil record, only two other instances are described of conifers that produced winged seeds that routinely included symmetric double-winged forms: the Paleogene Araucariacean *Doliostrobus* (Kvaček 2002) and Paleocene *Agathis*-like seeds (Escapa et al. 2013). Interestingly, just like *Manifera*, these taxa represent early occurrences of autorotating seed dispersal within their lineage. Also in these separate instances of autorotative wind dispersal evolution, the exclusively autorotating

dispersal syndrome seen later in these lineages may well have been the product of a similar multistep process.

Acknowledgments

We thank M. Gibson, former manager of the 6666 Ranch, for permission to work on ranch property, and J.-L. Wilde and L. Lyles for access to their property. D. Chaney and W. DiMichele are acknowledged for bringing Looy into the field and for many fruitful discussions. N. Nagalingum (Royal Botanic Gardens, Sydney) and H. Forbes (UC Botanical Garden at Berkeley) provided us with *Agathis* seeds. K. Calderwood and our Undergraduate Research Apprentice Program students at University of California, Berkeley (R. Ayala, A. Ayuby, M. Hao, F. Kusumo, K. Lee, and especially R. Balbin Uy) assisted with photographing, filming, and data collection. The Center for Integrative Biomechanics Education and Research (CIBER) is thanked for use of equipment. R. Dudley and Y. Zeng graciously provided additional equipment and a controlled space for drop tests. I. Duijnstee is acknowledged for discussions and help with data analysis and figure preparation. D. Contreras, S. P. Quek, D. Lentink, and two anonymous reviewers helped to improve our research project and this manuscript. This research was supported by the Hellman Fellowship, and the University of California Museum of Paleontology. This is University of California Museum of Paleontology Contribution number 2054.

Literature Cited

Augspurger, C. K. 1986. Morphology and dispersal potential of wind-dispersed diaspores of neotropical trees. American Journal of Botany 73:353–363.

Azuma, A., and Y. Okuno. 1987. Flight of a samara, *Alsomitra macrocarpa*. Journal of Theoretical Biology 129:263–274.

Azuma, A., and K. Yasuda. 1989. Flight performance of rotary seeds. Journal of Theoretical Biology 138:23–53.

Benkman, C. W. 1995. Wind dispersal capacity of pine seeds and the evolution of different seed dispersal modes in pines. Oikos 73:221–224.

Bergman, N. M., T. M. Lenton, and A. L. Watson. 2004. COPSE: a new model of biogeochemical cycling over Phanerozoic time. American Journal of Science 304:397–437.

Berner, R. A. 2009. GEOCARBSULF: Phanerozoic atmospheric oxygen: new results using the GEOCARBSULF model. American Journal of Science 309:603–606.

Burrows, F. M. 1975. Wind-borne seed and fruit movement. New Phytologist 75:405–418.

Call, V. B., and D. L. Dilcher. 1997. The fossil record of *Eucommia* (Eucommiaceae) in North America. American Journal of Botany 84:798–814.

Chaney, D. S., and W. A. DiMichele. 2007. Paleobotany of the classic redbeds (Clear Fork Group - Early Permian) of North Central Texas. Pp. 357-366 *In* T. Wong, ed. Proceedings of the XVth International Congress on Carboniferous and Permian Stratigraphy (Utrecht, 10-16 August 2003). Royal Netherlands Academy of Arts and Sciences, Amsterdam.

Childress, S., N. Vandenberghe, and J. Zhang. 2006. Hovering of a passive body in an oscillating airflow. Physics of Fluids 18:117103.

Clark, J. S. 1998. Why trees migrate so fast: confronting theory with dispersal biology and the paleorecord. American Naturalist 152:204–224.

Clement-Westerhof, J. A. 1984. Aspects of Permian palaeobotany and palynology. IV. The conifer *Ortiseia* Florin from the Val Gardena Formation of the Dolomites and Vicentinian Alps (Italy) with special reference to a revised concept of the Walchiaceae (Göppert) Schimper. Review of Palaeobotany and Palynology 41:51–166.

——. 1987. Aspects of Permian paleobotany and palynology, VII. The Majonicaceae, a new family of Late Permian conifers. Review of Palaeobotany and Palynology 52:375–402.

——. 1988. Morphology and phylogeny of Palaeozoic conifers. Pp. 298–337 *in* C. Beck, ed. Origin and evolution of gymnosperms. Columbia University Press, New York.

DiMichele, W. A., S. H. Mamay, D. S. Chaney, R. W. Hook, and J. W. Nelson. 2001. An Early Permian flora with Late Permian and Mesozoic affinities from north-central Texas. Journal of Paleontology 75:449–460.

DiMichele, W. A., N. J. Tabor, D. S. Chaney, and W. J. Nelson. 2006. From wetlands to wet spots: environmental tracking and the fate of Carboniferous elements in the Early Permian tropical floras. *In* S. F. Greb and W. A. DiMichele, eds. Wetlands through time. Geological Society of America Special Paper 399: 223–248.

Dudley, R. 1998. Atmospheric oxygen, giant Paleozoic insects, and the evolution of aerial locomotor performance. Journal of Experimental Biology 201:1043–1050.

Dudley, R., and P. Chai. 1996. Animal flight mechanics in physically variable gas mixtures. Journal of Experimental Biology 199:1881–1885.

Dudley, R., G. Byrnes, S. P. Yanoviak, B. Borrell, R. M. Brownand, and J. A. McGuire. 2007. Gliding and the functional origins of flight: biomechanical novelty or necessity? Annual Review of Ecology, Evolution, and Systematics 38:179–201.

Eckenwalder, J. E. 2009. Conifers of the world. Timber, Portland, Ore.

Eriksson, O., E. M. Friis, and P. Löfgren. 2000. Seed size, fruit size, and dispersal systems in angiosperms from the Early Cretaceous to the Late Tertiary. American Naturalist 156:47–58.

Escapa, I., A. Iglesias, P. Wilf, and N. Cuneo. 2013. Oldest macrofossil record of *Agathis* (Araucariaceae), early Paleocene of Patagonia, Argentina, and its evolutionary significance. Botanical Society of America 2013 Meeting, New Orleans, Louisiana, Abstracts, p. 378.

Evangelista, D. J. 2013. Aerial righting, directed aerial descent, and maneuvering in the evolution of flight in birds. Ph.D. thesis. University of California, Berkeley.

Evangelista, D., S. Hotton, and J. Dumais. 2011. The mechanics of explosive dispersal and self-burial in the seeds of the filaree, *Erodium cicutarium* (Geraniaceae). Journal of Experimental Biology 214:521–529.

Evangelista, D., S. Cam, T. Huynh, I. Krivitskiy, and R. Dudley. 2014a. Ontogeny of aerial righting and wing flapping in juvenile birds. Biology Letters 10:20140497.

Evangelista, D., S. Cam, T. Huynh, A. Kwong, H. Mehrabani, K. Tse, and R. Dudley. 2014b. Shifts in stability and control effectiveness during evolution of Paraves support aerial maneuvering hypotheses for flight origins. PeerJ 2:e632.

Farjon, A. 1990. Pinaceae. Koeltz Scientific Books, Koenigstein, Germany.

——. 2005. A monograph of Cupressaceae and *Sciadopitys*. Royal Botanic Gardens, Kew.

——. 2010. A handbook of the world's conifers. Brill Academic, Leiden, the Netherlands.

Givnish, T. J. 1980. Ecological constraints on the evolution of breeding systems in seed plants: dioecy and dispersal in gymnosperms. Evolution 34:959–972.

Graham, J. B., R. Dudley, N. M. Aguilar, and C. Gans. 1995. Implications of the late Palaeozoic oxygen pulse for physiology and evolution. Nature 375:117–120.

Green, D. S. 1980. The terminal velocity and dispersal of spinning samaras. American Journal of Botany 67:1218–1224.

Greene, D. F., and E. A. Johnson. 1989. A model of wind dispersal of winged or plumed seeds. Ecology 70:339–347.

——. 1990. The aerodynamics of plumed seeds. Functional Ecology 4:117–125.

——. 1992. Can the variation in samara mass and terminal velocity on an individual plant affect the distribution of dispersal distances? American Naturalist 139:825–838.

——. 1993. Seed mass and dispersal capacity in wind-dispersed diaspores. Oikos 67:69–74.

Greene, D. F., and M. Quesada. 1992. Seed size, dispersal, and aerodynamic constraints within the Bombacaceae. American Journal of Botany 92:998–1005.

Hedrick, T. L., B. Cheng, and X. Deng. 2009. Wingbeat time and the scaling of passive rotational damping in flapping flight. Science 324:252–255.

Horn, H. S., R. Nathan, and S. R. Kaplan. 2001. Long-distance dispersal of tree seeds by wind. Ecological Research 16: 877–885.

Howe, H. F., and M. N. Miriti. 2004. When seed dispersal matters. Bioscience 54:651–660.

Howe, H. F., and J. Smallwood. 1982. Ecology of seed dispersal. Annual Review of Ecology and Systematics 13:201–228.

Hughes, L., M. Dunlop, K. French, M. R. Leishman, B. Rice, L. Rodgerson, and M. Westoby. 1994. Predicting dispersal spectra: a minimal set of hypotheses based on plant attributes. Journal of Ecology 82:933–950.

Kerp, J. H. F., R. J. Poort, H. A. J. M. Swinkels, and R. Verwer. 1990. Aspects of Permian palaeobotany and palynology. IX. Conifer-dominated Rotliegend floras from the Saar-Nahe Basin (?Late Carboniferous–Early Permian; SW-Germany) with special reference to the reproductive biology of early conifers. Review of Palaeobotany and Palynology 62:205–248.

Kvaček, Z. 2002. Novelties on *Doliostrobus* (Doliostrobaceae), an extinct conifer genus of the European Palaeogene. Časopis Národního Muzea 171:131–175.

Labandeira, C. C. 2002. The history of associations between plants and animals. Pp. 26–74, 248–261 *In* C. Herrera, and O. Pellmyr, eds. Plant-animal interactions: an evolutionary approach, Blackwell Science, Oxford, England.

Lentink, D., W. B. Dickson, J. L. van Leeuwen, and M. H. Dickinson. 2009. Leading-edge vortices elevate lift of autorotating plant seeds. Science 324:1438–1440.

Leslie, A. B. 2011. Shifting functional roles and the evolution of conifer pollen producing and seed-producing cones. Paleobiology 37:587–602.

Leslie, A. B., J. M. Beaulieu, P. R. Crane, and M. J. Donoghue. 2013. Explaining the distribution of breeding and dispersal syndromes in conifers. Proceedings of the Royal Society B 280:20131812. doi:10.1098/rspb.2013.1812 [Epub ahead of print].

Levin, S. A., H. C. Muller-Landau, R. Nathan, and J. Chave. 2003. The ecology and evolution of seed dispersal: a theore tical perspective. Annual Review of Ecology, Evolution, and Systematics 34:575–604.

Looy, C. V. 2007. Extending the range of derived Late Paleozoic conifers: *Lebowskia* gen. nov. (Majonicaceae). International Journal of Plant Sciences 168:57–972.

Looy, C. V., and R. A. Stevenson. 2014. Earliest occurrence of autorotating seeds in conifers: the Permian (Kungurian-Roadian) *Manifera talaris* gen. et sp. nov. International Journal of Plant Sciences 175:841–854.

McCay, M. G. 2003. Winds under the rain forest canopy: the aerodynamic environment of gliding tree frogs. Biotropica 35:94–102.

McCutchen, C. W. 1977. The spinning rotation of Ash and Tulip Tree samaras. Science 197:691–692.

Meijering, O. D., and I. Smal. 2012. Methods for cell and particle tracking. Methods in Enzymology 504:182–200.

Minami, S., and A. Azuma. 2003. Various flying modes of wind-dispersal in seeds. Journal of Theoretical Biology 225:1–14.

Mirams, R. V. 1957. Aspects of the natural regeneration of the Kauri (*Agathis australis* Salish.). Transactions of the Royal Society of New Zealand 84:661–680.

Montañez, I. P., N. J. Tabor, D. Niemeier, W. A. DiMichele, T. D. Frank, C. R. Fielding, J. L. Isbell, L. P. Birgenheier, and M. C. Rygel. 2007. CO_2-forced climate and vegetation instability during Late Paleozoic deglaciation. Science 315:87–91.

Nathan, R., and H. C. Muller-Landau. 2000. Spatial patterns of seed dispersal, their determinants and consequences for recruitment. Trends in Ecology and Evolution 15:278–285.

Nathan, R., U. N. Safriel, and I. Noy-Meir. 2001. Field validation and sensitivity analysis of a mechanistic model for tree seed dispersal by wind. Ecology 82:374–388.

Nathan, R., G. G. Katul, H. S. Horn, S. M. Thomas, R. Oren, R. Avissar, S. W. Pacala, and S. A. Levin. 2002. Mechanisms of long-distance dispersal of seeds by wind. Nature 418:409–413.

Nathan, R., F. M. Schurr, O. Spiegel, O. Steinitz, A. Trakhtenbrot, and A. Tsoar. 2008. Mechanisms of long-distance seed dispersal. Trends in Ecology and Evolution 23:638–647.

Norberg, R. 1973. Autorotation, self-stability, and structure of single-winged fruits and seeds (samaras) with comparative remarks on animal flight. Biological Reviews 48:561–596.

Okubo, A., and S. A. Levin. 1989. A theoretical framework for data analysis of wind dispersal of seeds and pollen ecology 70: 329–338.

Owens, J. N., G. L. Catalano, and J. Aitken-Christie. 1997. The reproductive biology of Kauri (*Agathis australis*). IV. Late embryogeny, histochemistry, cone and seed morphology. International Journal of Plant Science 158:395–407.

Phillips, T. L., and W. A. DiMichele. 1992. Comparative ecology and life-history biology of arborescent lycopods in Late Carboniferous swamps of Euramerica. Annals of the Missouri Botanical Garden 79:560–588.

R Development Core Team. 2013. R: a language and environment for statistical computing. R Foundation for Statistical Computing, Vienna. http://www.R-project.org/.

Rothwell, G. W., G. Mapes, and G. R. Hernandez-Castillo. 2005. *Hanskerpia* gen. nov. and phylogenetic relationships among the most ancient conifers (Voltziales). Taxon 54:733–750.

Royal Botanic Gardens Kew. 2008. Seed information database (SID), Version 7.1. http://data.kew.org/sid/, accessed September 2013.

Schippers, P., and E. Jongejans. 2005. Release thresholds strongly determine the range of seed dispersal by wind. Ecological Modeling 185:93–103.

Schulz, C., P. Knopf, and T. H. Stützel. 2005. Identification key to the Cypress family (Cupressaceae). Feddes Repertorium 116: 96–146.

Sipe, T. W., and A. R. Linnerooth. 1985. Intraspecific variation in samara morphology and flight behavior in *Acer saccharinum* (Aceraceae). American Journal of Botany 82:1412–1419.

Soons, M. B., and J. M. Bullock. 2008. Non-random seed abscission, long-distance wind dispersal and plant migration rates. Journal of Ecology 96:581–590.

Tiffney, B. H. 1986. Evolution of seed dispersal syndromes according to the fossil record. Pp. 273–305 *in* D. R. Murray, ed. Seed dispersal. Academic Press, Sydney.

——. 2004. Vertebrate dispersal of seed plants through time. Annual Review of Ecology, Evolution, and Systematics 35:1–29.

Tiffney, B. H., and S. J. Mazer. 1995. Angiosperm growth habit, dispersal and diversification reconsidered. Evolutionary Ecology 9:93–117.

Uhl, D. 2007. Typification of the fossil conifer *Pseudovoltzia liebeana* (Geinitz) Florin. Taxon 53:185–186.

Van der Pijl, L. 1982. Principles of dispersal in higher plants. Springer, Berlin.

Varshney, K., S. Chang, and Z. J. Wang. 2012. The kinematics of falling maple seeds and the initial transition to a helical motion. Nonlinearity 25:C1–C8.

Wardlaw, B. R. 2005. Age assignment of the Pennsylvanian–Early Permian succession of North Central Texas. Permophiles 46:21–22.

Wickham, H. 2009. ggplot2: elegant graphics for data analysis. Springer, New York. http://had.co.nz/ggplot2/book.

Willson, M. F., and A. Traveset. 2000. The ecology of seed dispersal. Pp. 85–110 *in* M. Fenner, ed. Seeds: the ecology of regeneration in plant communities. CAB International, New York.

Yasuda, K., and A. Azuma. 1997. The autorotation boundary in the flight of samaras. Journal of Theoretical Biology 185:313–320.

Zeng, Y. 2013. Aerial righting, directed aerial descent and maneuvering in stick insects. Ph.D. thesis. University of California, Berkeley.